

N73-10032

NASA TECHNICAL
MEMORANDUM



NASA TM X-2652

NASA TM X-2652

CASE FILE
COPY

EFFECT OF DUCT SHAPE, MACH NUMBER,
AND LINING CONSTRUCTION ON
MEASURED SUPPRESSOR ATTENUATION
AND COMPARISON WITH THEORY

*by William A. Olsen, Jr., Eugene A. Krejsa,
and James W. Coats*

*Lewis Research Center
Cleveland, Ohio 44135*

1. Report No. NASA TM X-2652	2. Government Accession No.	3. Recipient's Catalog No.	
4. Title and Subtitle EFFECT OF DUCT SHAPE, MACH NUMBER, AND LINING CONSTRUCTION ON MEASURED SUPPRESSOR ATTENUATION AND COMPARISON WITH THEORY		5. Report Date November 1972	
		6. Performing Organization Code	
7. Author(s) William A. Olsen, Jr., Eugene A. Krejsa, and James W. Coats		8. Performing Organization Report No. E-7009	
		10. Work Unit No. 132-80	
9. Performing Organization Name and Address Lewis Research Center National Aeronautics and Space Administration Cleveland, Ohio 44135		11. Contract or Grant No.	
		13. Type of Report and Period Covered Technical Memorandum	
12. Sponsoring Agency Name and Address National Aeronautics and Space Administration Washington, D. C. 20546		14. Sponsoring Agency Code	
15. Supplementary Notes			
16. Abstract <p>Noise attenuation was measured for several types of cylindrical suppressors that use a duct lining composed of honeycomb cells covered with a perforated plate. The experimental technique used gave attenuation data that were repeatable and free of noise floors and other sources of error. The suppressor length, the effective acoustic diameter, suppressor shape and flow velocity were varied. The agreement among the attenuation data and two widely used analytical models was generally satisfactory. Changes were also made in the construction of the acoustic lining to measure their effect on attenuation. One of these produced a very broadband muffler.</p>			
17. Key Words (Suggested by Author(s)) Noise reduction Mufflers Acoustic ducts Noise suppressors		18. Distribution Statement Unclassified - unlimited	
19. Security Classif. (of this report) Unclassified	20. Security Classif. (of this page) Unclassified	21. No. of Pages 31	22. Price* \$3.00

* For sale by the National Technical Information Service, Springfield, Virginia 22151

CONTENTS

	Page
SUMMARY	1
INTRODUCTION	2
APPARATUS AND PROCEDURE	3
Acoustic Measurements	4
Procedure	5
Suppressor Geometry	7
Noise Source and Extraneous Noise	8
RESULTS AND DISCUSSION	11
Experimental Test Case Data	11
Discussion of Analyses	15
Description of analytical models	15
Choice of noise input for analyses	16
Comparison of Analytical and Experimental Attenuation Results	17
Idealized construction	17
Actual construction	19
The Effect of Changes in the Construction of the Acoustic Lining	19
Common cavity splitter	20
Cell to cell leakage	20
Back leakage and wideband suppressor	22
The Effect of Noise Generation Within the Suppressor	26
CONCLUDING REMARKS	26
APPENDIX - SYMBOLS	27
REFERENCES	29

EFFECT OF DUCT SHAPE, MACH NUMBER, AND LINING CONSTRUCTION ON MEASURED SUPPRESSOR ATTENUATION AND COMPARISON WITH THEORY

by William A. Olsen, Jr., Eugene A. Krejsa, and James W. Coats

Lewis Research Center

SUMMARY

Noise attenuation was measured for several types of cylindrical noise suppressors that use a duct lining composed of honeycomb cells covered with perforated plate. The noise source was a broadband aerodynamic noise that was produced by a small choked orifice far upstream of the suppressor. Sound-power-level attenuation spectra were obtained by the insertion loss technique using far-field microphone measurements. In this technique the noise passing through the acoustically lined suppressor is compared with that passing through the suppressor when it was taped (hard wall). Sound-pressure-level attenuation in the duct was also measured by placing flush mounted microphones upstream and downstream of the lined suppressor. Both attenuation methods gave essentially the same result. The experimental technique used was successful in giving attenuation spectral data that were repeatable and free of noise floors and other sources of error.

The main parameters studied were the suppressor length, effective acoustic diameter, suppressor shape, and flow velocity. These were varied without changes in the acoustic lining. The length and effective diameter were varied by changes in length and by the insertion of plugs and splitters. The Mach number was varied from 0.08 to 0.57. The measured attenuation spectra were compared with calculated results from two widely used analytical models. The agreement among the data and these analytical models was generally satisfactory. One of these models was also revamped to account for the actual construction of the suppressors (such as a distribution in the number of holes per honeycomb cell). The agreement with the data improved but not enough to warrant the increased analytical complexity.

The acoustic liner used in this study is made of perforated plate, honeycomb, and a solid backing sheet. Changes were made in the construction of this type of acoustic lining to determine their effect on performance. Openings can occur between the honeycomb cells of the acoustic lining for drainage and cooling or because of construction limitations. It was found that a 20-percent opening did not seriously reduce the attenuation performance. The solid backing sheet was replaced by perforated plate so that there was leakage through the back of the cell to the environment or a large volume. This produced a very broadband muffler.

INTRODUCTION

One proven way to reduce the turbomachinery noise of an aircraft engine is to acoustically treat the fan inlet and exhaust ducts (refs. 1 and 2) of the engine. In reference 3 jet noise was reduced by an acoustically lined ejector. Acoustically lined ducts are also used to reduce air conditioning machinery noise and the noise generated by valves. Part of the aircraft noise research program at Lewis Research Center involves experimental and analytical investigations of the acoustic performance of noise suppressors.

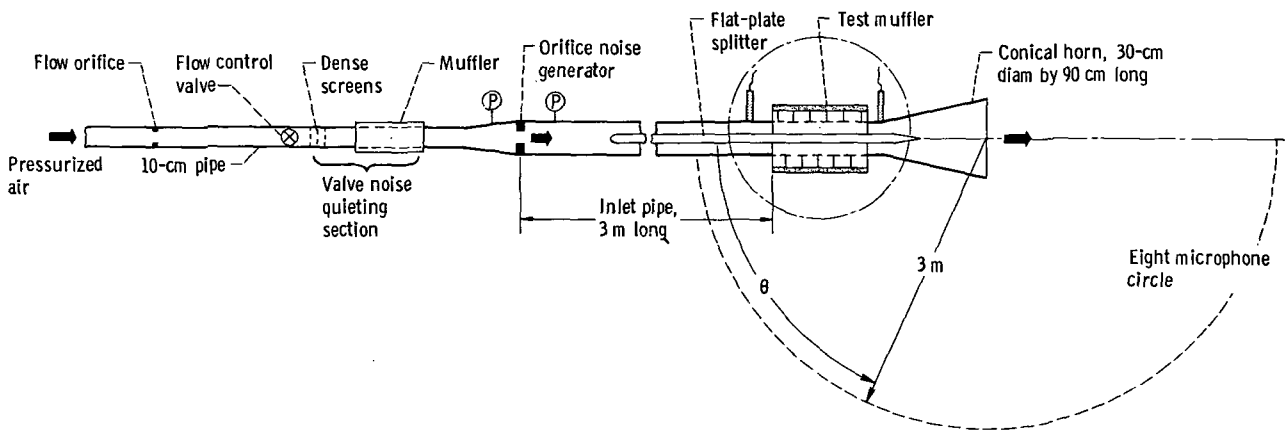
The acoustic lining in this study was the Helmholtz resonator type constructed of honeycomb cavities covered with perforated plate. The noise source was high-frequency broadband aerodynamic noise generated far upstream of the suppressor by a choked orifice. The flow and noise travel in the same direction. One purpose of this study was to provide experimental attenuation data with a broadband noise source. These data are then used as test cases for some analytical suppressor attenuation models. The main parameters varied were suppressor length and the effective acoustic diameter, suppressor shape, and flow velocity. These were generally varied without changing the acoustic lining. The length and effective acoustic diameter were varied by changes in length and by the insertion of plugs and splitters. The other purpose of this study was to determine the effect on performance of those variations in the acoustic lining that might occur in practical suppressor hardware. For example, what is the effect of openings between cells, and openings through the cell back to the environment or a large volume? What is the effect on suppression when the noise is generated within the muffler (e.g., a lined ejector)? An effort was also made to develop a wideband muffler.

The attenuation resulting from a given suppressor duct was determined by two independent techniques. In one method the sound power level passing through the suppressor duct to the environment was measured by a number of microphones in the far field. By comparing the resulting sound-power-level spectrum with that obtained when the suppressor acoustic lining was taped (hard-wall case) the insertion loss attenuation was obtained. In the other technique the sound pressure level at the duct wall was measured upstream and downstream of the suppressor. The difference in these sound-pressure-level spectra is the noise reduction when corrected for the small difference in readings when the suppressor is taped.

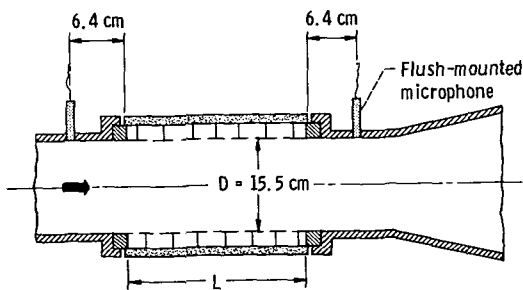
Analytical results from the models described in references 4 to 6 were compared with experimental results. These analyses used the same suppressor dimensions, duct Mach number, and noise input. It was then ascertained which of the measured noise inputs would give the best agreement between theory and experiment. Small changes to one of the analytical models were also made to account for the fact that the suppressors tested departed somewhat from a theoretical design. For example, they did not have a fixed number of holes per cavity, and some of the treated area was not acoustically effective.

APPARATUS AND PROCEDURE

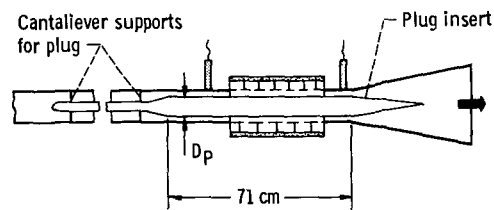
Figure 1 is a sketch and figure 2 contains a photograph of the test apparatus. Proceeding downstream from the inlet (fig. 1), there is a flow measurement orifice, a flow control valve, a valve noise quieting section, an orifice noise generator, a 20-diameter inlet pipe followed by the test suppressor, and a conical horn termination to the environment. Splitters and plugs can be placed in the suppressor duct to change effective acoustic diameter and shape of the suppressor as shown in figure 1.



(a) Flow system and test muffler shown with flat-plate splitter insert.



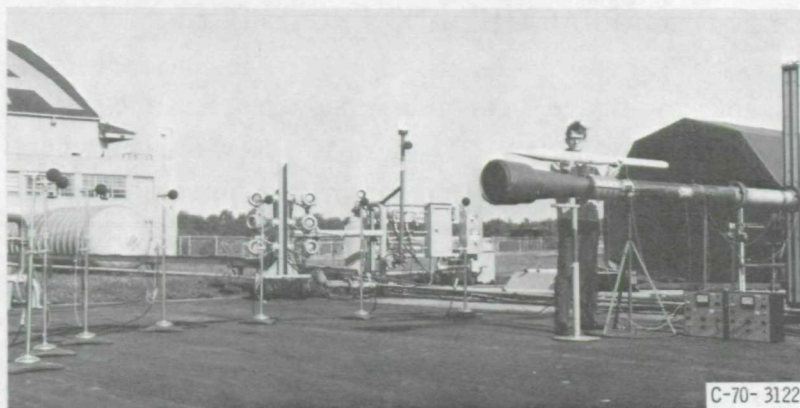
(b) Test muffler with no insert.



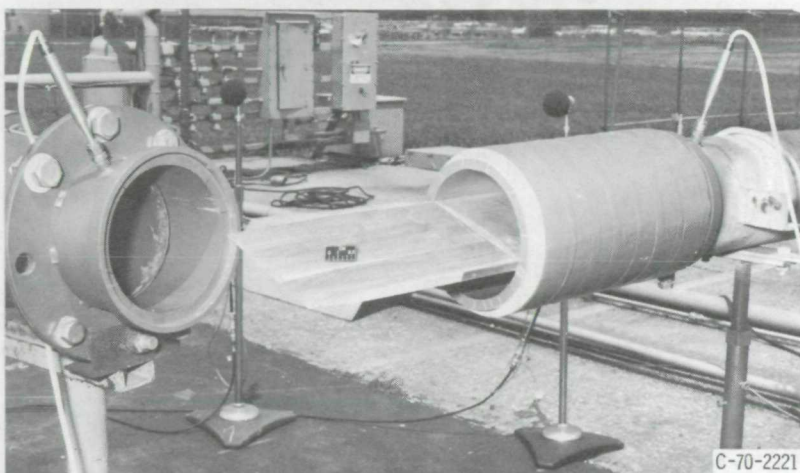
(c) Test muffler shown with cylindrical plug insert.

CD-11336-02

Figure 1. - Experimental apparatus.



(a) Experimental test setup with the axial location of plug insert indicated.



(b) Suppressor taken apart to show hard wall (internally taped) cylinder with splitter.

Figure 2. - Photographs of the experimental apparatus.

Acoustic Measurements

The objective of the experimental program was to obtain the noise attenuation spectra of various suppressor configurations. The attenuation was determined by two independent attenuation measurement methods. The first method uses eight 1.27-centimeter (1/2-in.) condensor microphones (with windscreens) that are placed on a 3-meter semi-circle centered around the horn exit. The eight microphones are located in a horizontal plane that passes through the nozzle centerline. The centerline is 1.2 meters above a smooth flat asphalt surface. The sound-power-level spectrum, PWL (symbols defined in the appendix) of noise passing through the suppressor duct was calculated from the sound-pressure-level spectra measured by the eight microphones. When the acoustically treated walls of the suppressor are exposed to the noise it is called the soft-wall case. When the suppressor surface is taped, so that it can no longer attenuate the noise, it is

called the hard-wall case. The attenuation (insertion loss) spectrum is the difference between the hard- and soft-wall power spectra (ref. 7, pp. 434-437).

Two flush mounted 0.63-centimeter (1/4-in.) microphones, one upstream of the suppressor and one downstream (fig. 1(b)), were used to obtain the other measurement of attenuation. The attenuation spectrum in this case (noise reduction) is the difference between the resulting upstream and downstream sound-pressure-level spectrum. A small correction to this attenuation was made for the small apparent attenuation spectrum (positive and negative) when the muffler is taped. This correction was less than ± 2 decibels in the frequency range of interest.

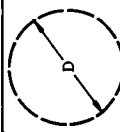
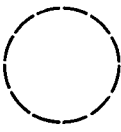
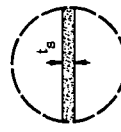
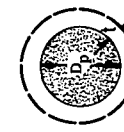
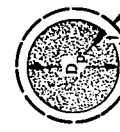
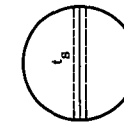
Procedure

The test procedure was to set up a given suppressor configuration and obtain the soft- and hard-wall noise data, described in a previous section, at a given flow and input noise condition. Three noise data samples were taken from each microphone at each run condition. Noise data were analyzed directly by a one-third-octave band spectrum analyzer. The analyzer determined sound-pressure-level spectra, referenced to 2×10^{-5} newtons per square meter. The three samples were then arithmetically averaged. In the case of the far-field data a correction was applied for the microphone and cable system losses and also for atmospheric losses. From these averaged and corrected spectra (SPL), the sound power spectrum (PWL), used in determining the insertion loss, was calculated. In the case of the two flush-mounted microphones the long cables and intense noise levels in the duct necessitated an impedance matching device. This involved an additional amplifier that was used to drive each cable. With this arrangement no microphone-cable correction was needed.

All the microphones were calibrated before each day of running with a standard piston calibrator (a 124-dB tone at 250 Hz). The one-third-octave band analyzer was calibrated before each days run with a constant voltage and checked during the experiment with an electronic pink noise generator. In addition, the whole system (from the microphones through the data analysis) was further checked with an independent external orifice noise source, which is known to be repeatable to about 1.5 decibels. Considering these calibrations and checks, repeated data, and the averaging of three samples widely spaced in time, the reported data should be repeatable to within 2 decibels for data taken on different days. Most comparisons were taken on the same day where the repeatability was within 1 decibel.

TABLE I. - SUPPRESSOR DIMENSIONS, SIZES, AND CONDITIONS

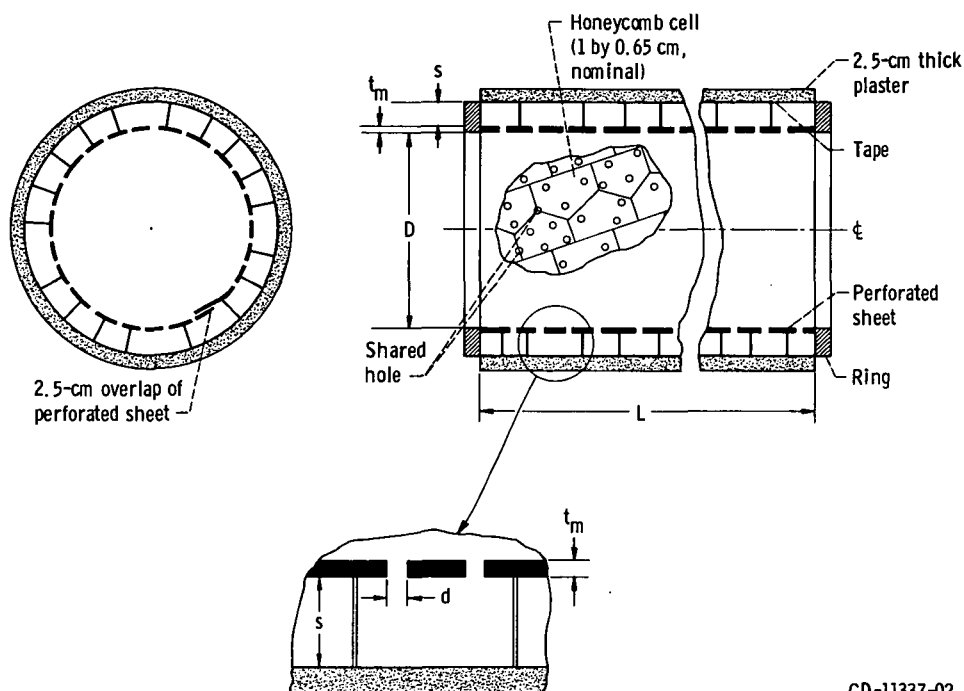
[Duct diameter, D, 15.5 cm; percent open area in perforated plate, σ , 8; plate thickness, t_m , 0.054 cm; plate hole diameter, d, 0.127 cm.]

Suppressor dimensions and shape											Calculated parameters			Experimental conditions		Attenuation plotted in figs. -
Type of suppressor	Duct length, L, cm	Annular gap, t, cm	Splitter thickness, t _s ' cm	Plug diameter, D _p ' cm	Backing distance, s, cm	Effective acoustic diameter, D', cm	Effective length to diameter ratio, L/D'	Ratio of treated surface to cross-sectional area, S/A	(S/A)(4L/D')	Duct Mach number (nominal), M	Noise input, OASPL _{wall} , dB					
	Cylinder, L/D'=1	15	---	----	--	0.8	D' = D = 15.5	≈ 1	$\frac{\pi DL}{\pi D^2} = \frac{4L}{D}$	1.0	0.08	162	5(b), 7(b)			
	Cylinder, L/D'=2	30	---	----	--	0.8	D' = D = 15.5	≈ 2	$\frac{\pi DL}{\pi D^2} = \frac{4L}{D}$	1.0	0.08	162	5(a), 7(a)			
	Hard splitter	30	1.27	--	0.8	D' = D - t _s = 14.2	≈ 2	$\frac{(\pi D - 2t_s)L}{\pi D^2 - Dt_s^2}$	0.965	0.08	162	7(c)				
	10-cm plug	30	2.5	----	10	0.8	D' = 2t = 5	≈ 6	$\frac{\pi DL}{\pi D^2 - \frac{\pi(D - 2t)^2}{4}}$	0.6	0.12	160	7(d)			
	13-cm plug	30	1.3	----	13	0.8	D' = 2t = 2.5	≈ 12	$\frac{\pi DL}{\pi D^2 - \frac{\pi(D - 2t)^2}{4}}$	0.6	$\left\{ \begin{matrix} 0.22 \\ 0.57 \end{matrix} \right\}$	160	$\left\{ \begin{matrix} 8(a) \\ 8(b) \end{matrix} \right\}$			
	Splitter in hard-walled cylinder	30	1.27	--	0.475	D' = D - t _s = 14.2	≈ 2	$\frac{2DL}{\pi D^2 - Dt_s^2}$	0.65	0.08	162	7(e)				

Suppressor Geometry

Attenuation data were taken on two types of suppressors. The first type of suppressors tested involved changes in the suppressor length, effective acoustic diameter, and suppressor shape, while not changing the acoustic lining (see table I). Most of these runs were at very low duct Mach number ($M < 0.1$). A few runs were made with this acoustic lining at a high duct velocity. The first type of suppressors will be used as test cases for some analytical models. The second type of suppressor tests involved changes in the acoustic lining construction. These changes are described in a later section.

Figure 3 is a schematic that shows the construction of the first type of suppressors. In all cases (see table I) the cylindrical acoustical lining consisted of an 8-percent-open-area perforated plate, which was 0.054-centimeter thick with 0.127-centimeter-diameter holes. This cylindrical plate was glued to a honeycomb cell structure that formed cavities 0.8-centimeter deep and about 1 by 0.65 centimeter in cross section. The acoustic lining of the double celled splitter used the same perforated plate but the honeycomb had a different depth (0.475 cm deep).



CD-11337-02

Figure 3. - Suppressor dimensions and construction. Actual hardware discrepancies from idealized construction of table I: Percentage of holes shared by adjacent honeycomb cells, 35 percent; distribution of holes per cell: three (28 percent), four (20 percent), and five (43 percent); lost suppressor surface area due to lengthwise overlap of perforated plate and honeycomb butt joint, 5 percent.

These dimensions are for an idealized construction that could not be achieved exactly. As described in figure 3 the actual construction was somewhat different. There were holes shared by cavities and a distribution of holes per cavity. There was also a 5-percent loss in effective lining area because of a lengthwise perforated plate lap joint and a honeycomb butt joint.

Noise Source and Extraneous Noise

Figure 4(a) contains a plot of the sound-pressure level spectrum at the wall, SPL_{wall} , generated by a single orifice noise source (2.2-cm diam) at a pressure ratio of 8.8 across the orifice. This spectrum was measured by the flush mounted microphones when the acoustic lining of the cylindrical suppressor was taped (hard-wall case). The same spectrum results for the upstream mike when the tape was removed (soft-wall case). Figure 4(a) also contains the mean sound-pressure-level spectrum across the taped duct \overline{SPL}_{duct} . This is obtained from the sound power spectrum PWL that was calculated from the far-field sound data, by the following relation (ref. 7, pp. 53 and 179-180)

$$\overline{SPL}_{duct} = PWL - 10 \log(A_{duct}) - 9.8$$

Where A_{duct} is in square meters. This equation assumes that all the sound energy in the duct passes through to the environment. This is discussed in more detail further on in this section.

Floors caused by external noise that cannot be attenuated by the suppressor are a serious problem when an engine is used as the noise source for a test suppressor (ref. 8). The flow and acoustic measurement system was designed so that the significant attenuation of the suppressor occurred at frequencies far removed from all sources of noise other than the orifice noise source in the pipe. The center frequency of the orifice noise source is near the frequency of maximum suppressor attenuation. This matching is important for suppressors of large attenuation because the dynamic range of the noise data acquisition system is limited to a maximum of about 40 to 50 decibels. The noise generated by flow, without the orifice noise source installed, would be valve noise, internal flow noise, and jet noise. The first is at high frequency, and the last two occur at low frequency. Only the jet noise is an external noise that cannot be attenuated by the test suppressor. Valve noise, which was heavily attenuated upstream of the orifice noise source, in any event, was not a problem for this experiment because nearly all the pressure drop occurred at the orifice noise source. Figure 4(a) shows that the maximum attenuation occurs at frequencies well above the low-frequency noise caused by the jet exhausting through the horn (below 200 Hz). The combined noise from

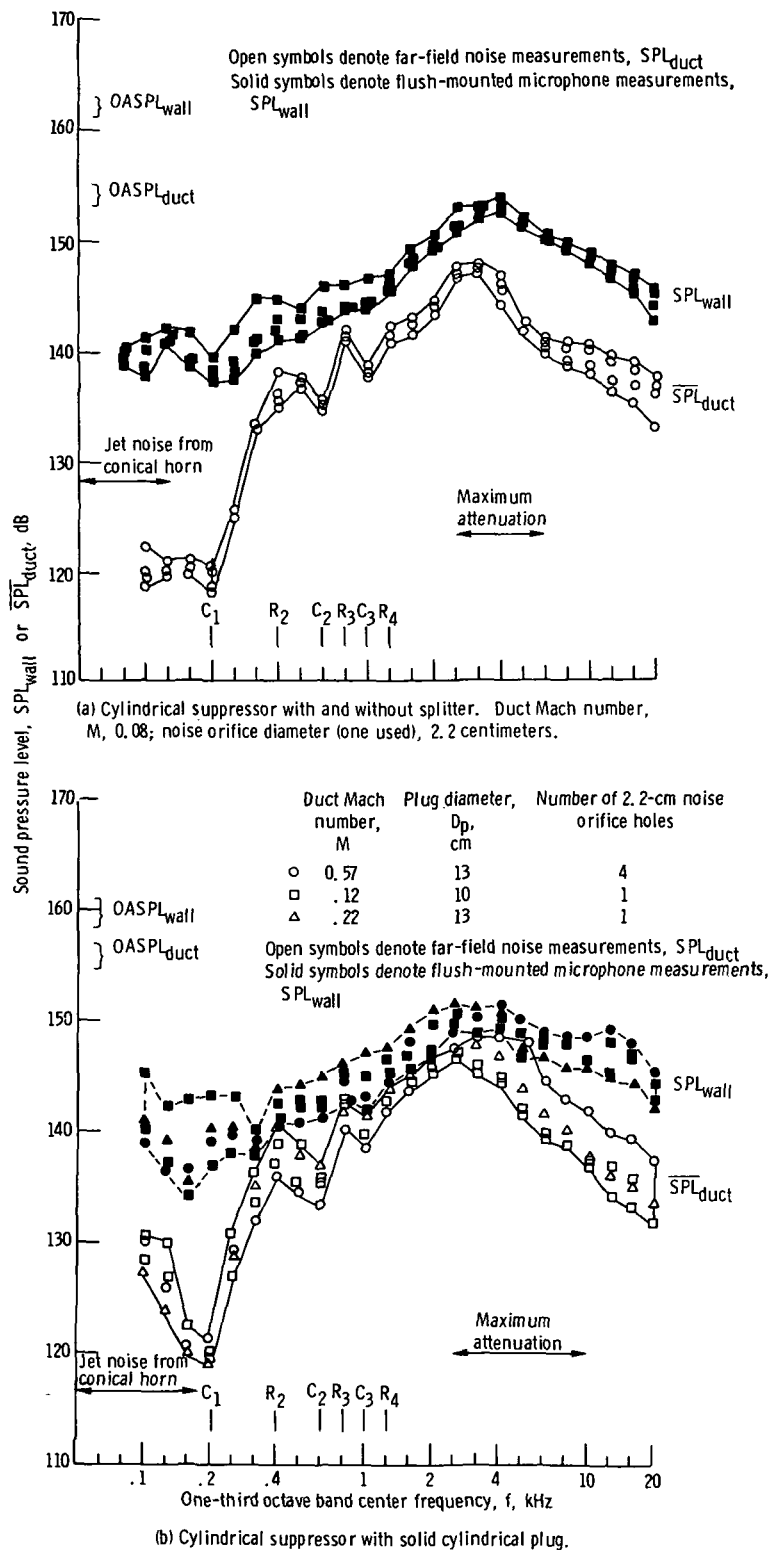


Figure 4. - Noise spectra from noise generation orifices used in this report. All acoustic surfaces are taped over. Duct diameter, D , 15.5 centimeters; duct length, L , 30 and 15 centimeters. Far-field ground reflection cancellation and reinforcement frequencies, C_i and R_i , respectively.

valve noise and internal flow noise above 200 hertz was estimated to be below $\overline{\text{SPL}}_{\text{duct}} = 110$ decibels. This means that jet, valve, and flow noise did not set a floor to the attenuation measurements of this report. Noise radiation through the pipe walls to the far field microphones was checked, and it was found that this was not a problem in these runs either. General background noise was also low enough that it too would not be a floor to the maximum measurable attenuation. In any case the suppressors tested were expected to not exceed a 20- to 30-decibel peak attenuation.

There are also reflection errors to consider. For the far-field microphones ground reflections must be considered. The cancellation and reinforcement frequencies are denoted by C_i and R_i in figure 4(a). But as is shown in figure 4(a) the far-field noise data that would be affected is well below the frequency of peak attenuation. The far-field and flush-mounted mikes are also affected by internal reflections brought about by the acoustic circuit, where the conical horn is the limiting element of that circuit. According to reference 9 the internal reflections for a conical horn of this size are large only below 400 hertz. But with a conical horn there is still a small loss even at the high frequency of peak attenuation.

In figure 4(b) a plug was used to decrease the effective acoustic diameter (resulting in higher attenuation) and increase the velocity through the suppressor. In this case the jet noise and internal flow noise increase somewhat, as is evidenced by the increase in $\overline{\text{SPL}}_{\text{duct}}$ below 200 hertz. But these external noise sources are still of very low level and low frequency and, therefore, cause no error. More orifice holes were required to pass the high flows corresponding to the higher velocities of figure 4(b). In spite of this, the noise level changed only slightly from the low-velocity cylindrical cases of figure 4(a).

The question arises as to why figure 4(a) shows that the sound-pressure-level spectra from the flush-mounted microphones SPL_{wall} is higher than the $\overline{\text{SPL}}_{\text{duct}}$ from the far-field microphones. At low frequency this is largely due to internal reflections, caused by the conical horn, and ground reflections. At high frequency you must consider two possible causes. As discussed before, it is partly due to the small loss from the internal reflections caused by the conical horn. The other part of the difference is probably related to the cutoff frequencies of the hard-wall duct between the orifice noise source and the suppressor. Reference 10 points out that, when the cutoff frequency of a mode is exceeded by the frequency of the sound in the duct, then that mode of sound can pass down the hard-wall duct with little attenuation. For the duct of figure 4(a) the cutoff frequencies (in Hz) for the various modes are

$$f_{0,0} = 0 \quad f_{1,0} = 1300 \quad f_{2,0} = 2200$$

$$f_{0,1} = 2750 \quad f_{3,0} = 3100$$

Since the noise source peaks at about 3 to 4 kilohertz, it is clear that practically all of

these modes exist in the suppressor duct. Therefore, it can be expected that SPL_{wall} would exceed \overline{SPL}_{duct} . This situation occurs for practical engine suppression ducts.

Turn now to figure 4(b) where the two spectra come closer together. Here the cutoff frequencies are much higher because of the small annular gap. For the 13-centimeter plug with the 1.3-centimeter annular gap, the cutoff frequencies (in Hz), calculated from the tables in reference 11 are about

$$f_{0,0} = 0 \quad f_{1,0} = 5500 \quad f_{0,1} = 72\,000$$

In this case far less modes can exist, and the radial variation of SPL would be much less. Therefore, \overline{SPL}_{duct} would approach SPL_{wall} near the peak noise frequencies. The question of which SPL should be used in an analysis is discussed in a later section.

The previous discussion has shown that reasonably accurate suppressor attenuation data can be achieved with the broadband noise source and apparatus described in this report, so long as the significant attenuation occurs from about 1 to 10 kilohertz. This is because these frequencies are far removed from common sources of error and those noise sources that cannot be attenuated by the suppressor. The suppressor configurations described in figure 3(a) have their significant attenuation at frequencies that fit this requirement. In the last part of this report some results for a wideband suppressor will be reported. This suppressor is able to attenuate noise pretty much across the whole spectrum. But these results will be subject to the errors at low frequency as described before and are therefore only useful in comparisons.

RESULTS AND DISCUSSION

Experimental Test Case Data

This section contains the experimental attenuation data to be used as test cases for some analytical suppressor performance models. The main parameters that were varied (as shown in table I) were suppressor length, effective acoustic diameter, suppressor shape, and duct Mach number. These variations were made without changing the acoustic lining, and the noise input was essentially unchanged (fig. 4). These results are compared with the attenuation predicted by two analyses.

Figure 5(a) is a plot of the insertion loss (IL) and noise reduction (NR) data (three runs of three samples each) for an $L/D' = 2$ (30-cm long) cylindrical suppressor at a low duct Mach number ($M = 0.08$). Figure 5(b) is a similar plot (for two runs) for an $L/D' = 1$ (15-cm long) cylindrical suppressor at the same conditions of flow and noise input. Both share the same acoustic lining, which is described in figure 3 and table I.

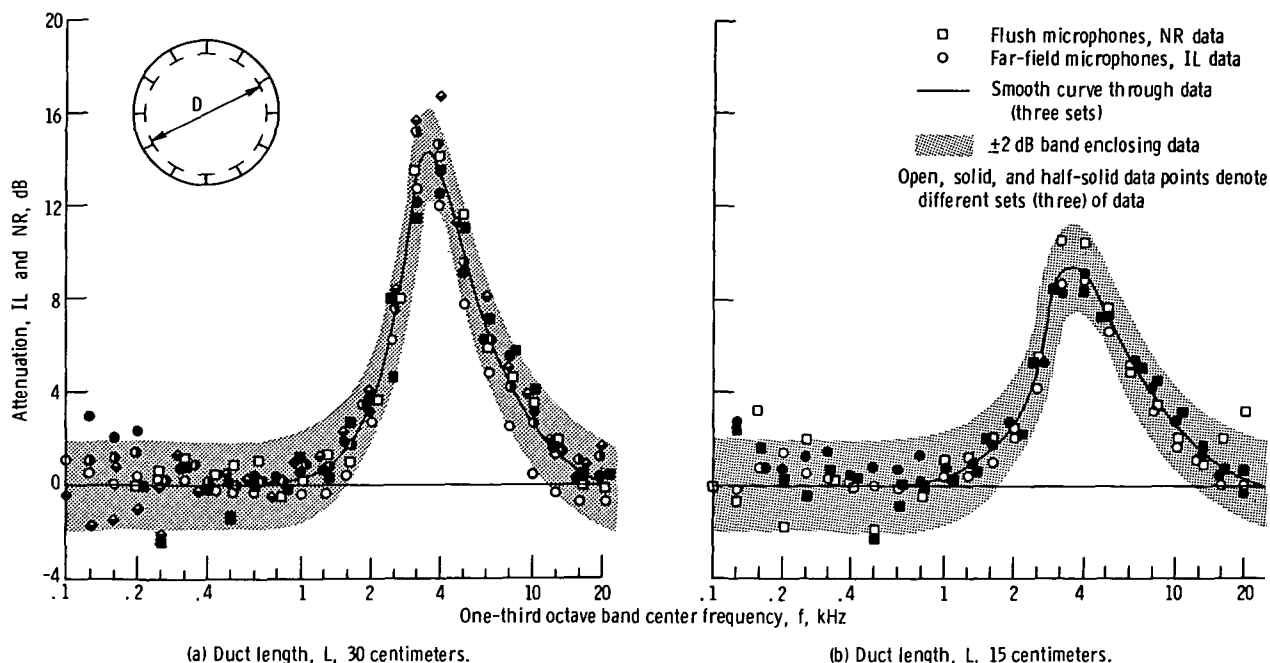


Figure 5. - Measured suppressor attenuation data for cylinder with no insert. Noise input, $OASPL_{wall}$, 162 decibels; Mach number, M , 0.08; open area in perforated plate, 8 percent; plate thickness, t_m , 0.054 centimeters; hole diameter, d , 0.127 centimeters; honeycomb backing distance, s , 0.8 centimeter; duct diameter, D , 15.5 centimeters.

A smooth curve was faired through the data and ± 2 decibel bands from the curves are indicated. The ± 2 decibel bands enclose most of the data. Figure 5 shows that the attenuation measured by the flush microphones NR agrees well with that measured with the far-field microphones IL.

Figure 6 is a plot of the far-field noise ($OASPL$) variation with the microphone angle θ for the hard wall version of the suppressor described in figure 5(a). The peak

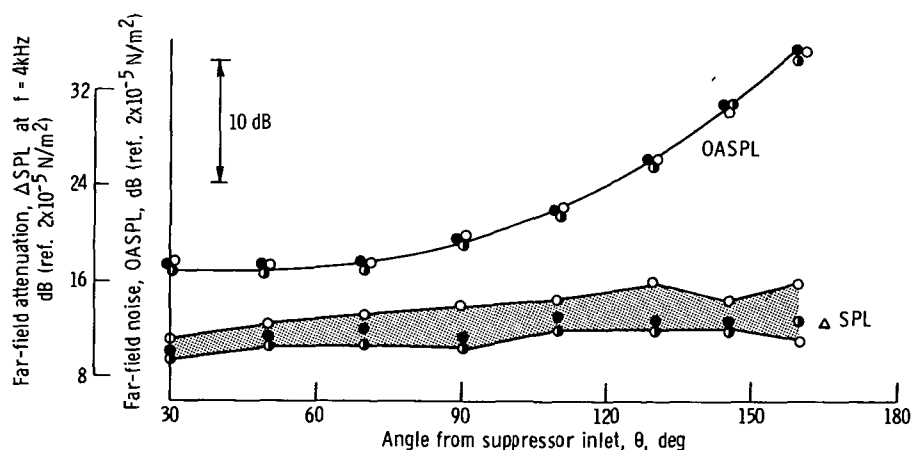
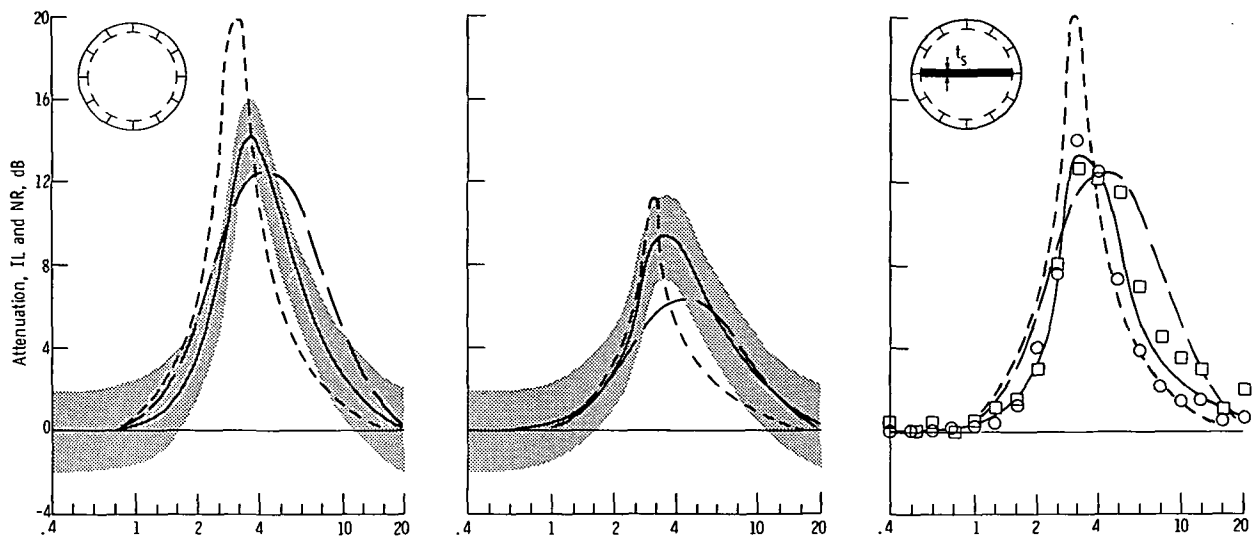


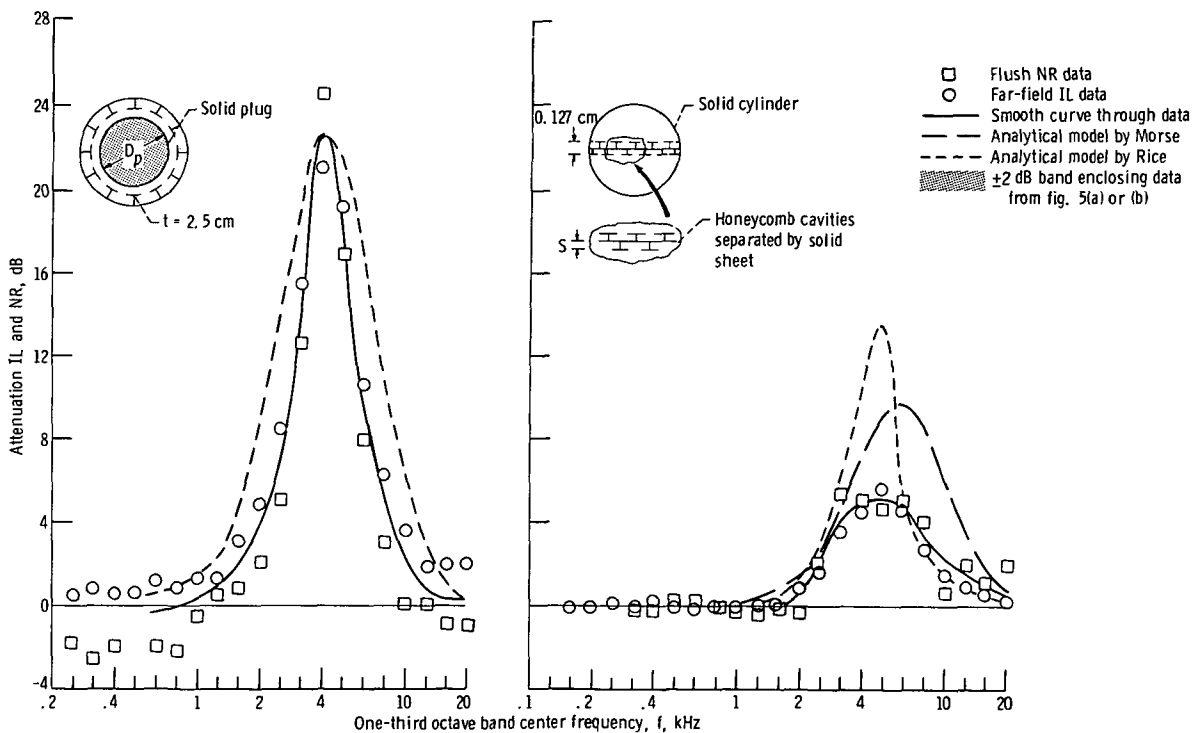
Figure 6. - Far-field noise radiation pattern (hard wall) and peak attenuation pattern in far field for three sets of data in figure 5(a).



(a) Cylindrical suppressor with no insert; duct length, L , 30 centimeters; Mach 0.08; honeycomb backing distance, s , 0.8 centimeter; noise input, $OASPL_{wall}$, 162 decibels.

(b) Cylindrical suppressor with no inserts; duct length, L , 15 centimeters; Mach 0.08; honeycomb backing distance, s , 0.8 centimeter; noise input, $OASPL_{wall}$, 162 decibels.

(c) Cylindrical suppressor with hard-wall splitter; splitter thickness, t_s , 1.27 centimeters; duct length, L , 30 centimeters; Mach 0.08; honeycomb backing distance, s , 0.8 centimeter; noise input, $OASPL_{wall}$, 162 decibels.



(d) Cylindrical suppressor with solid plug; plug diameter, D_p , 10 centimeters; duct length, L , 30 centimeters; Mach 0.12; honeycomb backing distance, s , 0.8 centimeter; noise input, $OASPL_{wall}$, 160 decibels.

(e) Hard-wall cylinder with separate cavity splitter suppression; splitter thickness, t_s , 1.27 centimeters; duct length, L , 30 centimeters; Mach 0.08; honeycomb backing distance, s , 0.475; noise input, $OASPL_{wall}$, 162 decibels.

Figure 7. - Measured attenuation and comparison with analytical prediction for cylindrical suppressor with and without inserts at low duct Mach numbers. Percent open area in perforated plate, 8; plate thickness, t_m , 0.054 centimeter; hole diameter, d , 0.127 centimeter; duct diameter, D , 15.5 centimeters.

noise and peak attenuation occur at about 4000 hertz. The variation of attenuation with θ at that frequency is also plotted in figure 6. The attenuation changed about 3 decibels, while the far-field noise varied about 18 decibels around the microphone circle. It is interesting that the peak attenuation did not vary much compared with the far-field noise variation. Perhaps it is because there were no noise floors, such as that caused by jet noise.

Figure 7(a) to (d) contain another set of test-case data where the L/D' was varied from 1 to 6 by changing the inserts installed in a 15.5-centimeter-diameter cylindrical suppressor. The inserts were a hard-wall splitter and hard-wall cylinders. The acoustic lining of the cylinder was not changed, and the noise input and duct Mach number

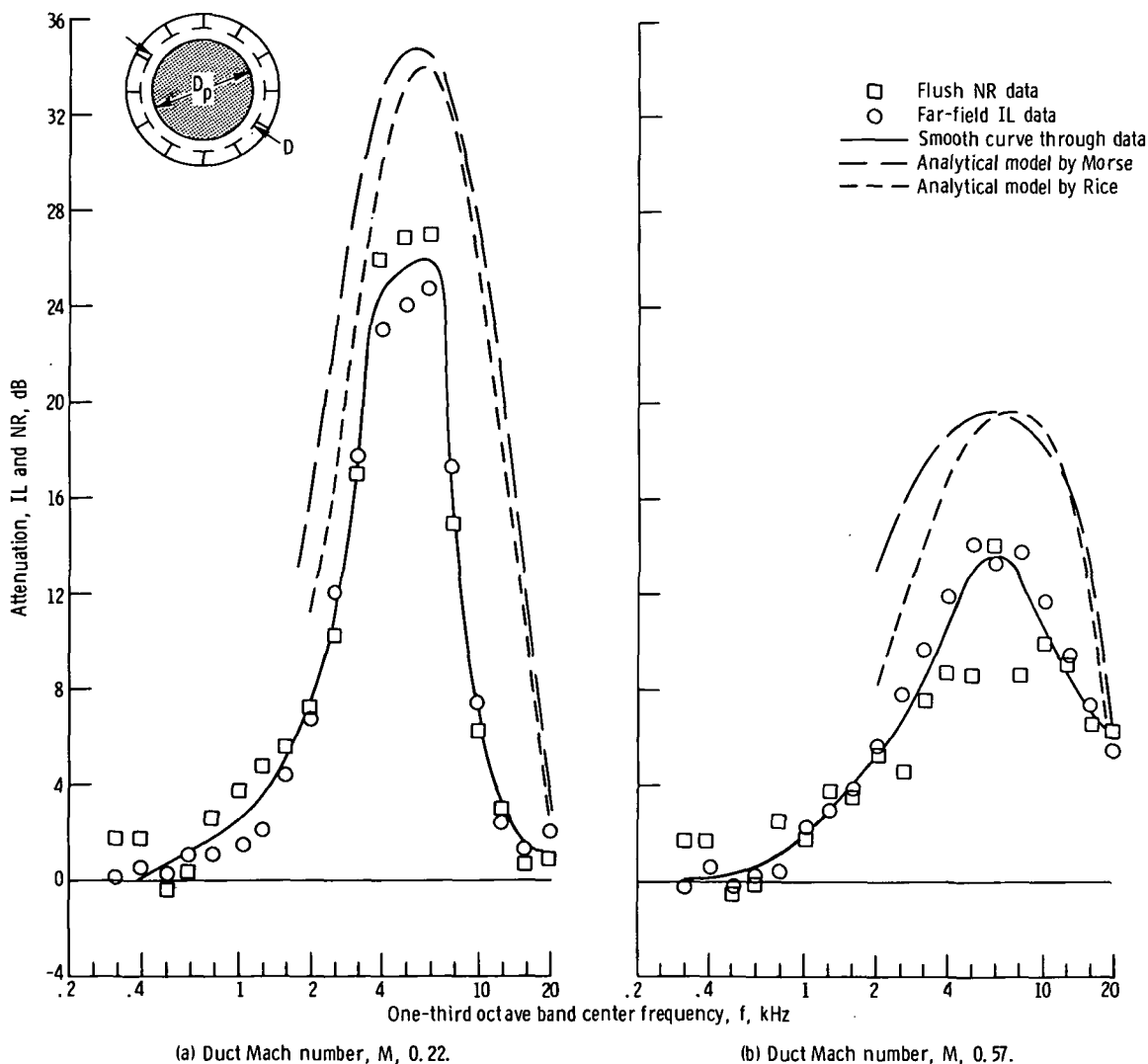


Figure 8. - Effect of duct Mach number on suppression attenuation. Standard suppressor (see fig. 5(a)) with solid plug. Plug diameter, 13 centimeters; duct length, L , 30 centimeters; duct diameter, D , 15.5 centimeters; honeycomb backing distance, s , 0.8 centimeter; percent open area in perforated plate, 8; plate thickness, t_m , 0.054 centimeter; hole diameter, d , 0.127 centimeter; Mach 0.08; noise input, $OASPL_{wall}$, 160 decibels.

were essentially the same. In figure 7(e) the acoustically lined cylinder was taped and a soft-wall splitter of different design was installed (see table I). Figure 8 contains the attenuation spectra for a cylindrical duct with a hard-wall cylindrical plug that results in an annular gap of 1.25 centimeters. Figure 8(a) contains the spectra for a duct Mach number of 0.22; figure 8(b) is for a duct Mach number of 0.57. The NR data and IL attenuation data in figures 7 and 8 are again in good agreement.

Discussion of Analyses

Description of analytical models. - Two analytical models are described in this section. Results from these analyses will be compared in a subsequent section with the data for the test cases reported in the previous section. Either model can be considered to consist of two parts. The first part deals with the propagation of sound in an acoustically lined duct. The second part deals with the specification of the boundary conditions, in particular, the acoustic impedance of the acoustic liner. The solution to the propagation equation, which involves the acoustic impedance of the liner, is a transcendental equation. It has an infinite number of solutions representing the modes that may exist in the duct. The basic difference between the two analytical models compared in this report is the way this equation is solved and the way the modes are used. Rice (ref. 4) solves this equation for the first 10 eigenvalues. These models are then used together to initially form a plane pressure wave at the lined duct entrance. Morse (ref. 6) derived approximations to all the modes. However, suppressor attenuation is typically calculated by using only the first eigenvalue (Morse's approximate model), which results in a valid solution for hard or nearly hard walls. The solutions from Rice's model and Morse's approximate model would tend to agree when the wall impedance is large or when the effective acoustic diameter of the duct is small compared with the wavelength of the sound (i. e., small D'/λ).

A cylindrical duct analysis was used for all the analytical comparisons regardless of the shape of the duct. Attenuation for the noncylindrical cases are obtained by analyzing a cylinder of some effective acoustic diameter. The effective acoustic diameter was taken to be the maximum distance between absorbing surfaces, or twice the maximum distance between the absorbing surface and a reflecting surface. The geometries tested and the parameters used in the analyses are shown in table I.

The wall impedance model reported by Groeneweg (ref. 5) is used to define the impedance boundary condition needed for both of the propagation models. Groeneweg's wall impedance model considers the effect of grazing flow Mach number on the resistance and reactance of the acoustic liner. The effect of a noise spectrum (and finite pressure amplitude effects) are approximated by using the overall sound pressure level of the

noise. Any errors in this impedance model will affect the results from the two propagation models.

Choice of noise input for analyses. - The analytical attenuation models require the specification of the sound pressure inside the suppressor. Figure 4 shows that the OASPL in the duct is somewhat different depending on how it was measured. The average overall sound pressure level across the duct, which was measured by the far-field microphones $\overline{\text{OASPL}}_{\text{duct}}$, is lower than the level for the flush mounted microphones $\text{OASPL}_{\text{wall}}$. In figure 4(a) where the input noise spectrum for the cylindrical suppressors is plotted, $\text{OASPL}_{\text{wall}} = 162$ decibels and $\overline{\text{OASPL}}_{\text{duct}} = 154$ decibels. For the higher attenuation plug inserts, the input noise spectrum is plotted in figure 4(b), and $\text{OASPL}_{\text{wall}} = 160$ decibels and $\overline{\text{OASPL}}_{\text{duct}} = 156$ decibels. The question is which measurement should be used ($\text{OASPL}_{\text{wall}}$ or $\overline{\text{OASPL}}_{\text{duct}}$), or does it really matter. Since

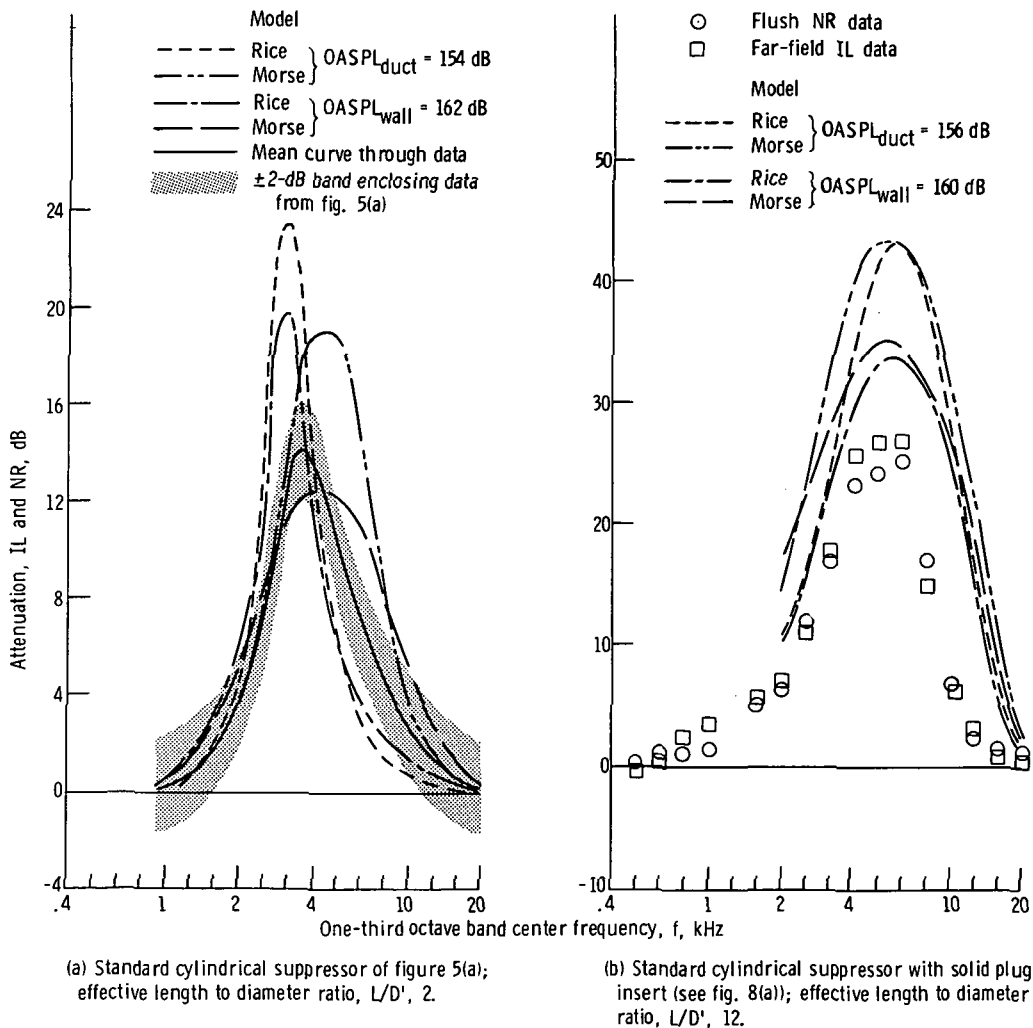


Figure 9. - Comparison of analytical attenuation results, evaluated at $\overline{\text{OASPL}}_{\text{duct}}$ and $\text{OASPL}_{\text{wall}}$ by two models, with experimental data.

the wall impedance is determined by the pressure at the wall, the $OASPL_{wall}$ would appear to be the better choice. The analytically determined attenuation for the two models considered is plotted in figure 9(a) for a cylindrical suppressor ($L/D' = 2$) at the two measured input noise levels ($OASPL_{duct}$ and $OASPL_{wall}$). Figure 9(b) shows the same comparison for an $L/D' = 12$ suppressor. The choice of noise input level has some affect for both suppressors. From figure 9 it can be seen that the analytical results using the $OASPL_{wall}$ are in somewhat better overall agreement with the data. In most practical cases either choice of $OASPL$ would probably be adequate. But, to be consistent, the comparisons among the data and analytical results that follow will be made at the $OASPL_{wall}$ value.

Comparison of Analytical and Experimental Attenuation Results

The analytical acoustic suppressor models require uniform steady flow into the duct and a plane pressure wave at the inlet. With the noise generating orifice far upstream of the muffler, a turbulent velocity profile (nearly uniform) would be achieved in the pipe. But no noise surveys were taken across the duct; therefore, it is not known if a plane pressure wave existed at the inlet. What will prove interesting, on looking ahead, is how well these highly simplified analytical models predict the attenuation that was actually measured.

Idealized construction. - References 1 and 8 made comparisons between analytical and experimental results. In these studies the experimental value of $OASPL_{duct}$ was used, and the analytical models assumed that the wall impedance of a suppressor liner was spatially uniform. Comparisons between theory and experiment will be made first for all the test cases in order to supply an overall impression. Based on the previous section the $OASPL_{wall}$ will be used instead of $OASPL_{duct}$. Plotted in figures 7(a) to (d) are the attenuation spectrum for four suppressors of varying L/D' at a low duct Mach number. They share the same acoustic liner (see table I for details). Figures 7(a) and (b) contain the mean curve and bands enclosing the data on figures 5(a) and (b), respectively.

The analytical attenuation prediction of the Rice model is compared with the data. The predicted frequency of peak attenuation generally agrees with the data, and the overall spectra agreement is favorable. The actual attenuation spectra are generally broader than predicted by this model. Figure 7(e) is for a hard-wall cylinder with an acoustically lined splitter (see description in table I). The agreement is not as favorable in this case, probably because this geometry is not adequately approximated by a cylinder of an equivalent acoustic diameter. Figure 8 contains similar comparisons with the theory but at high duct Mach numbers. The overall agreement is, again, satisfactory.

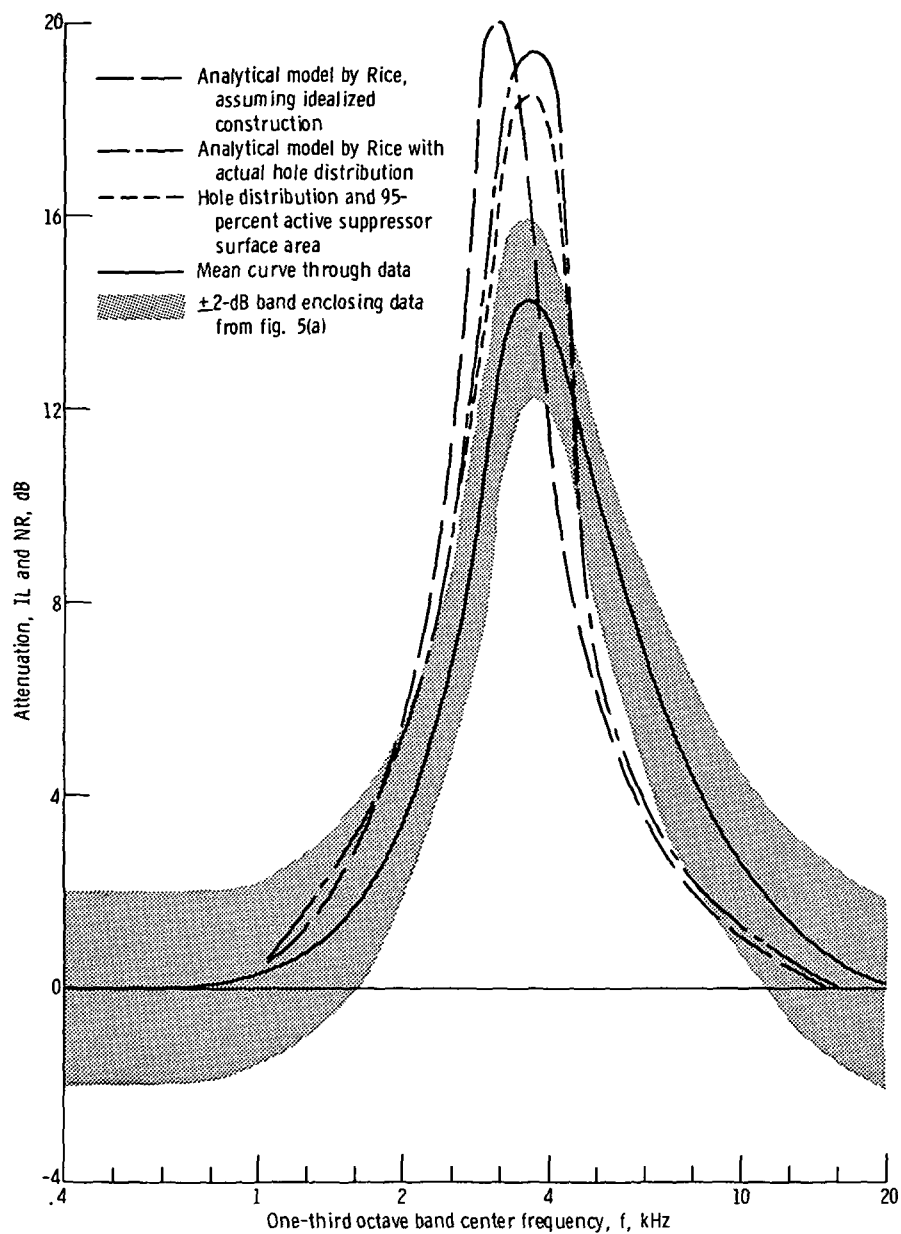


Figure 10. - Change in analytical attenuation prediction when actual construction of suppressor is considered.

The analytical results for Morse's approximate model are also plotted in figures 7 and 8. The analytical results of the Rice model are quite different from Morse's model except at small D'/λ , where they come together. The overall agreement between Morse's approximate model and these data is about as good as the agreement with Rice's model. For these test cases Morse's model tends to give a broader attenuation spectrum than that measured. The attenuation spectrum from Rice's model tends to be narrower than that measured.

Actual construction. - In the preceding comparisons it was assumed that the suppressor linings were of idealized construction. But in reality (as described in fig. 3), the suppressor linings were necessarily made with a distribution of holes per cavity. And only about 95 percent of the surface area was active because of losses caused by lengthwise joints of the perforated plate and of the honeycomb. The more general Rice model was revamped to give some idea of the effect on attenuation of these departures from idealized construction. Figure 10 contains the predicted attenuation spectra, for the suppressor considered in figure 7(a), where the actual construction has been considered. To handle the distribution of holes per cavity, an equivalent lining impedance was determined. The impedance of a single cavity - perforated-plate combination was calculated as a function of the number of holes in the perforated plate. Then the parallel circuit impedance of all cavity - perforated-plate combinations was calculated taking into account the percentage at which the number of holes per cavity occurred. For comparison the analytical prediction from figure 7(a) for idealized construction is also plotted in figure 10. The frequency of peak attenuation has moved closer to that of the data, but the attenuation spectrum is still too narrow. Let us now consider the effect of having only 95 percent of the acoustic lining surface area as active. Multiply the attenuation spectrum achieved by considering the hole distribution by 0.95 (the active fraction of the liner). The resulting attenuation spectrum would be for a suppressor where the actual lining construction is considered. The agreement is slightly better. This 95-percent correction can be applied to the rest of the analytical curves in figures 7 and 8 if the reader wishes to do so.

The Effect of Changes in the Construction of the Acoustic Lining

The effect on measured attenuation of certain desirable variations in the construction of the suppressor lining is discussed in this section. For example, what is the effect of openings between honeycomb cells and openings through the cell back to the environment? What is the effect of generating noise within the suppressor? And can an acoustically lined splitter be made thinner? These effects are determined experimentally without any comparison with theory.

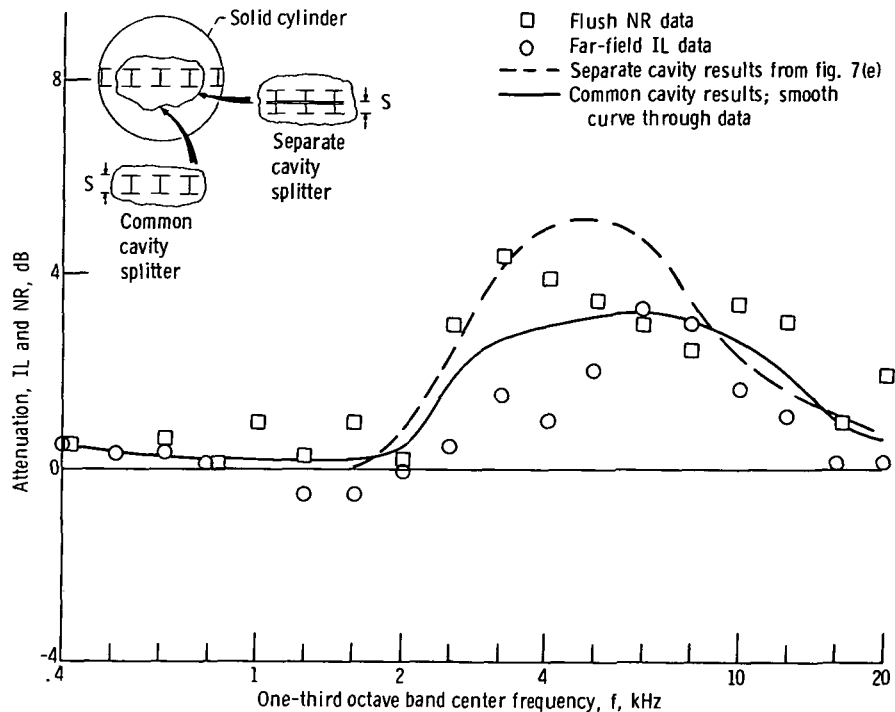


Figure 11. - Reduction in attenuation achieved by separate cavity splitter in solid cylinder when one cavity is used in common. Duct diameter, D , 15.5 centimeters; duct length, L , 30 centimeters; percent open area in perforated plate, 8; plate thickness, t_m , 0.054 centimeter; hole diameter, d , 0.127 centimeter; noise input, $OASPL_{wall}$, 162 decibels; duct Mach 0.08; splitter honeycomb backing distance, s , 0.48 centimeter.

Common cavity splitter. - Acoustically lined splitters may be used extensively in engine inlets and exits to reduce the noise radiation to the environment. The thickness of the splitter could be cut in half if the attenuation of a common cavity liner was nearly as good as the standard separate cavity liner. The common cavity liner type of splitter would be perforated plate on either side of the honeycomb structure so that the honeycomb cell volumes are shared by the perforated plate orifices on either side (see fig. 11). The separate cavity type of splitter would use two such honeycomb structures separated by a solid sheet. Figure 11 contains the attenuation spectrum data for these splitters. For comparison, the mean curve of the attenuation spectrum for the separate cavity splitter was copied from figure 7(e). There is a decrease in the attenuation in using the thinner common cavity splitter. However, the attenuation is too small for an accurate comparison.

Cell to cell leakage. - Cell to cell leakage will occur in practical honeycomb acoustic liners. Drainage slots are one cause, and the bond between the honeycomb, back sheet, and perforated plate is never perfect. In addition, some suppressor applications require openings for cooling. Do the honeycomb cell volumes have to be well sealed volumes in order to achieve good attenuation? To answer this question, a 0.16-

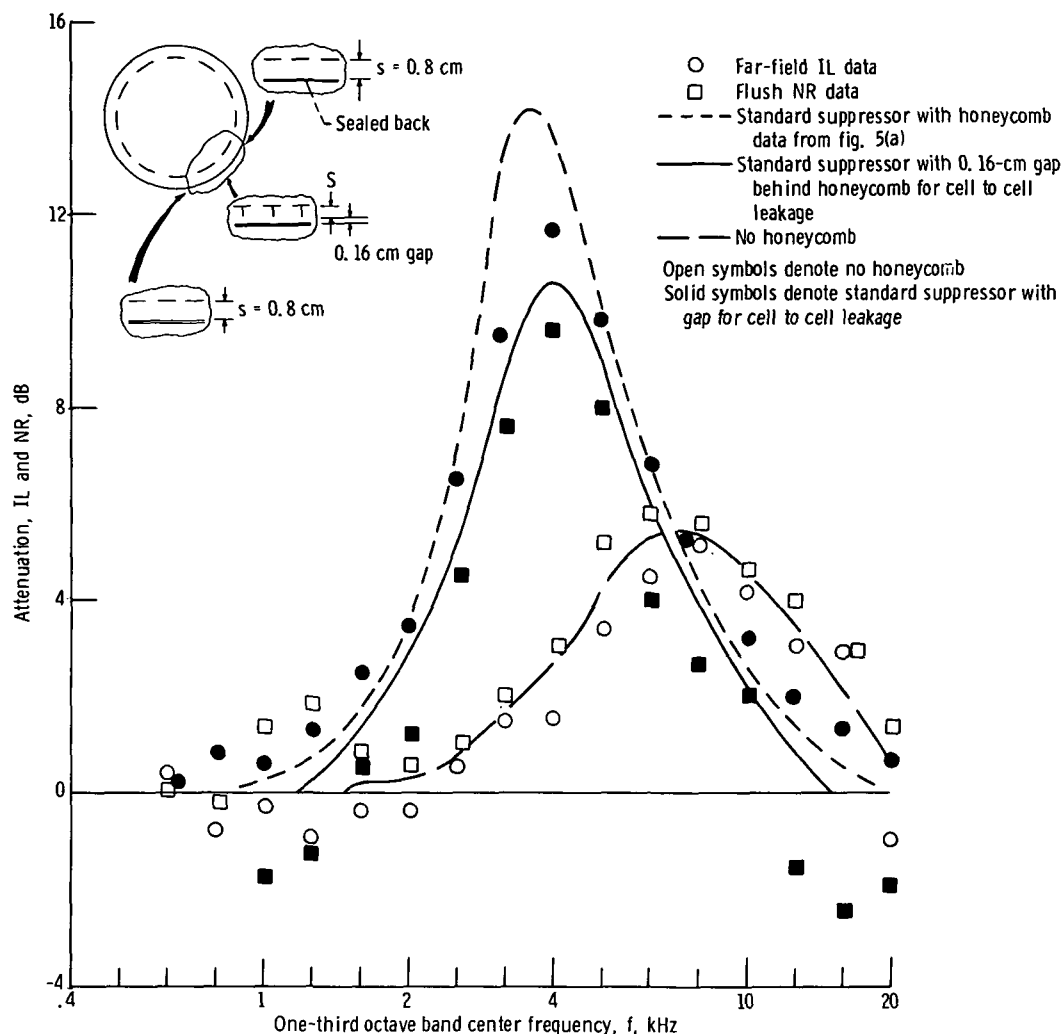


Figure 12. - Effect of honeycomb cell to cell leakage on attenuation. Standard suppressor (see fig. 5(a)); duct length, L , 30 centimeters; duct diameter, D , 15.5 centimeters; honeycomb backing distance, s , 0.8 centimeter; percent open area in perforated plate, 8; plate thickness, t_m , 0.054 centimeter; hole diameter, d , 0.127 centimeter; Mach 0.08; noise input, $OASPL_{wall}$, 162 decibels.

centimeter gap (20 percent in the honeycomb depth) was made between the solid back sheet and the honeycomb cell as shown in figure 12. The attenuation was reduced only a small amount by this large cell to cell leakage. Therefore, the performance of a suppressor designed for this frequency range would certainly not be significantly reduced by the smaller cell to cell leakage that would result from imperfect construction or drainage slots. Suppose there were no honeycomb cells (i. e., full cell to cell leakage). The attenuation (as evidenced by fig. 12) is reduced significantly in this case. The void between the perforated plate and impervious back sheet was then loosely filled with steel wool (packing density, 1.24 g/cm^3 ; wire diameter, $7.6 \times 10^{-4} \text{ cm}$). Figure 13 indicates that the attenuation was about the same as for the standard honeycomb cell construction.

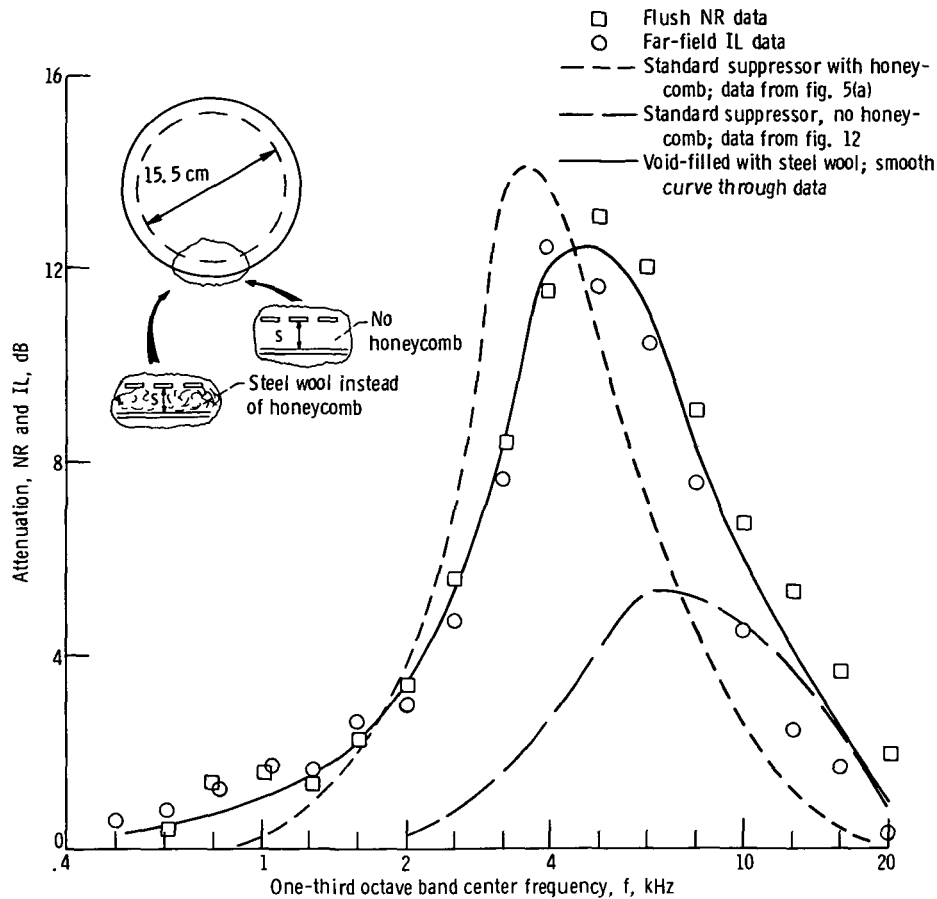


Figure 13. - Effect of removing honeycomb and then filling the void with steel wool. Backing distance, s , 0.8 centimeter; steel wool wire diameter, 7.6×10^{-4} centimeter; steel wool packing density, 1.24 grams per cubic centimeter; percent open area in perforated plate, 8; plate thickness, t_p , 0.054 centimeter; plate hole diameter, d , 0.127 centimeter; noise input, $OASPL_{wall}$, 162 decibels; duct Mach number, M , 0.08.

Back leakage and wideband suppressor. - Suppose the solid backing sheet had holes in it so that noise could leak out to the environment or a large sealed volume. The impedance of this type of suppressor is described by two coupled equations (i. e., two degrees of freedom). In these tests the suppressor was well within the microphone circle so that the far-field IL attenuation would also include the noise radiated through the suppressor wall that had holes in it. Figure 14 contains the attenuation spectrum mean data curve for a standard sealed back suppressor (from fig. 5(a)) and data for four variations where there is back leakage. Consider first the fully open back in figure 14(a). Here, real attenuation IL occurs in the far field only at low frequency. The large apparent attenuation "NR," measured by the flush microphones, indicates that considerable sound passes through the perforated plate to the environment. If any of the microphones were in the near field at these low frequencies, the IL attenuation measured here would be too low. The back leakage was then restricted with felt and the

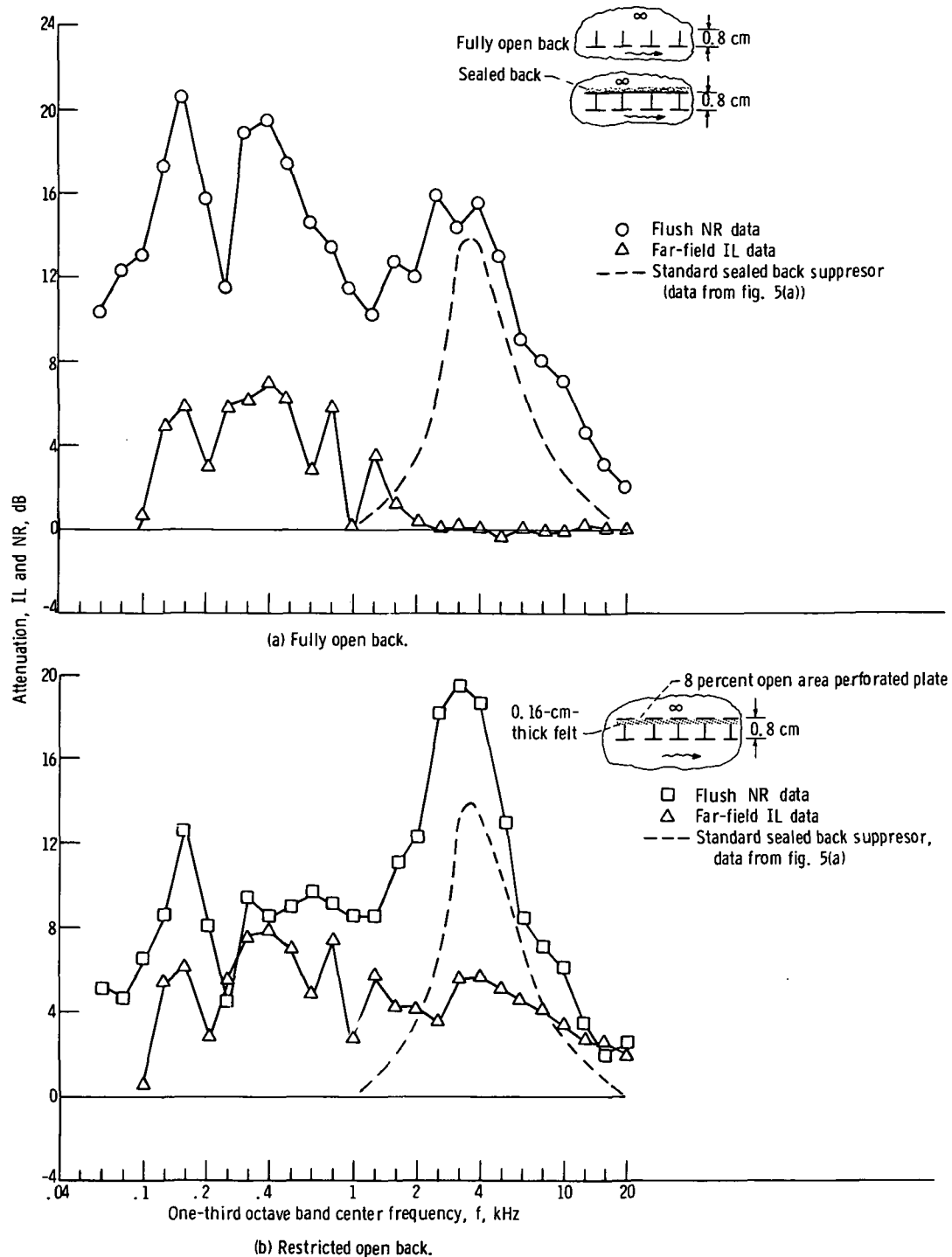


Figure 14. - Effect of leakage through back of acoustic liner. Duct length, L , 30 centimeters; duct diameter, D , 15.5 centimeters; honeycomb backing distance, s , 0.8 centimeter; percent open area in perforated plate, $\&$; plate thickness, t_m , 0.054 centimeter; hole diameter, d , 0.127 centimeter; Mach 0.08; noise input, $OASPL_{wall}$, 162 decibels.

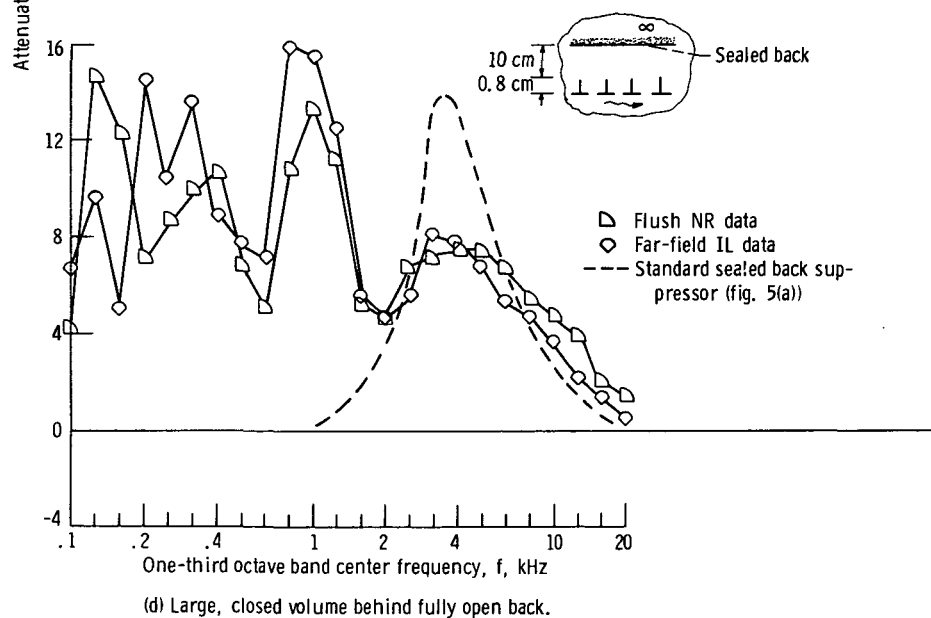
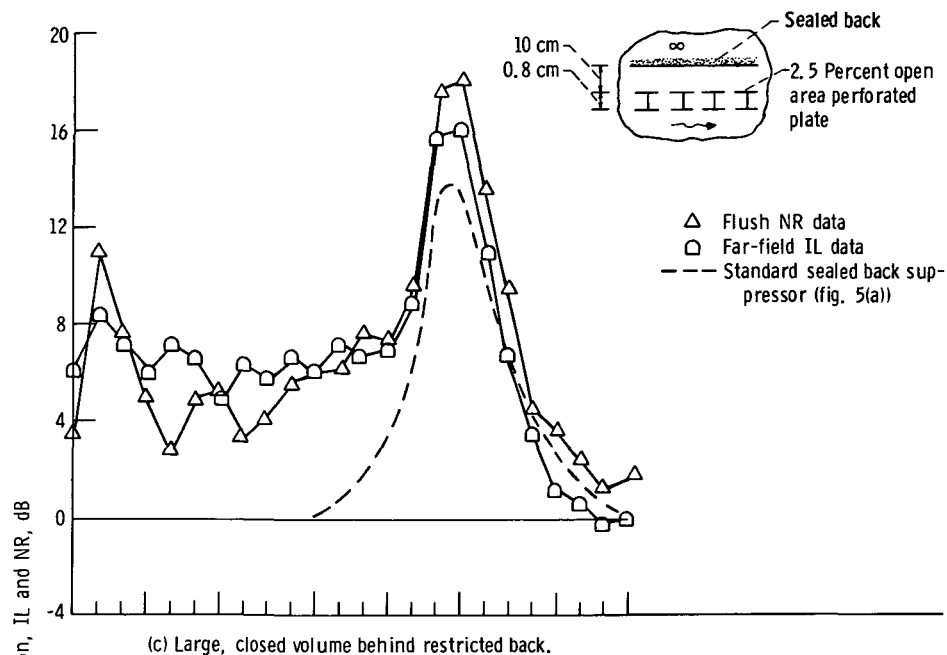


Figure 14. - Concluded.

same perforated plate as on the inside diameter of the suppressor. The far-field IL attenuation spectrum shown in figure 14(b) became more or less uniform, at about 5 decibels, from 100 hertz to 10 kilohertz. Considerable high-frequency sound still passed through to the environment as evidenced by the difference between the IL spectrum and the flush mike "NR" spectrum. In the next change a large, closed volume was placed behind this type of restricted back (as shown in fig. 14(c)). In this case the low-frequency attenuation remained essentially the same as for the restricted open back. But the high-frequency attenuation became about the same as for the standard hard backed suppressor. Also note that the far-field IL attenuation agrees well with the NR attenuation in this case where no noise can pass through the suppressor lining to the environment. In the final change the restricted back was removed (fig. 14(d)). The low-frequency attenuation improved but the high-frequency attenuation decreased.

The restricted open back and restricted back with a closed volume behind it may indicate practical ways to make very wideband suppressors. Keep in mind that these

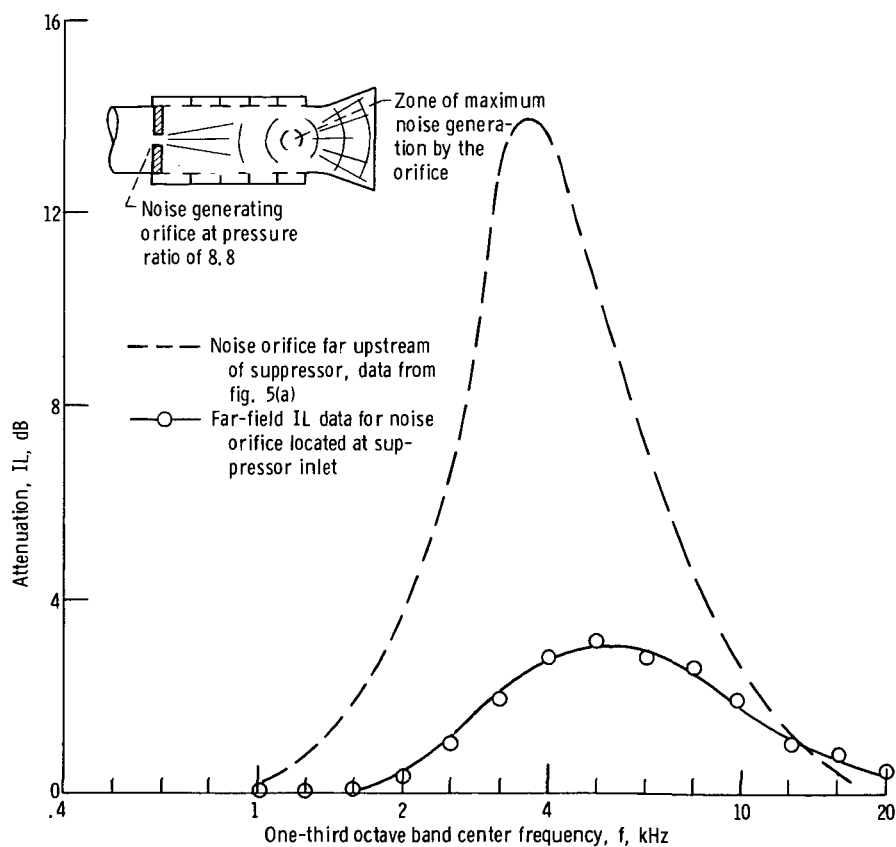


Figure 15. - Effect of generating noise inside suppressor with noise orifice moved downstream to suppressor inlet. Duct length, L , 30 centimeters; duct diameter, D , 15.5 centimeters; honey-comb backing distance, s , 0.8 centimeter; percent open area in perforated plate, 8; plate thickness, t_m , 0.05 centimeter; hole diameter, d , 0.127 centimeter; Mach 0.08; noise input, $OASPL_{wall}$, 162 decibels.

particular suppressors were not optimized acoustically. The restricted open back suppressor could be useful for ejectors where wideband attenuation is desired without a large back cavity.

The Effect of Noise Generation Within the Suppressor

All the previous data were taken with the orifice noise source far upstream of the test suppressor. The orifice noise source is now moved down to the inlet of the suppressor and run at the same pressure ratio. Figure 15 shows that the attenuation is greatly reduced from when the noise is generated far upstream. The reason for this is that much of the noise is generated near the exit of the suppressor as shown by the sketch in figure 15. This maximum noise generation location is based on data reported in reference 12.

CONCLUDING REMARKS

1. The suppressor attenuation spectra measurement technique used herein gave repeatable data that were free of noise floors and other common sources of error. The attenuation spectra obtained from either far-field or flush-mounted microphones are essentially the same.

2. The suppressor attenuation analytical model of Rice and the approximate model of Morse were in general agreement with the data. The same wall impedance model was used in both analyses. It was found that these models had somewhat better agreement with the data when the noise input of the flush mounted microphones was used.

3. The wall impedance model was revamped to account for the actual construction of the suppressors. This improved the agreement but not enough to warrant the increased analytical complexity.

4. Changes were made in the construction of the acoustic lining to determine their effect on performance. A significant amount of leakage from cell to cell did not seriously reduce the attenuation performance. Leakage through the back of the cell to the environment or a large, closed volume produced a two degree of freedom suppressor. This suppressor had a very broadband attenuation spectrum.

Lewis Research Center,
National Aeronautics and Space Administration,
Cleveland, Ohio, July 28, 1972,
132-80.

APPENDIX - SYMBOLS

A_{duct}	cross sectional area of duct within suppressor, m^2
C_1, C_2, C_3	ground reflection cancellation frequencies, Hz
D	duct diameter, m
D'	effective acoustic diameter, m
D_p	plug insert diameter, m
d	diameter of holes in perforated plate, m
f	one-third octave band center frequencies, Hz
$f_{0,0}, f_{1,0}$ $f_{2,0}, f_{0,1}$ }	cutoff frequencies for modes in a hard-wall cylindrical duct: plane wave, two for spin-radial, and radial, Hz
IL	insertion loss; difference between hard- and soft-wall power spectra (measured in the far field) dB
L	length of suppressor, m
M	Mach number within suppressor duct
NR	noise reduction; difference between the SPL_{wall} measured upstream and downstream of suppressor (a correction is then made for this differ- ence with hard walls), dB
"NR"	apparent NR because of noise leakage through the back of the suppres- sor, dB
OASPL	overall sound pressure level, dB
$\overline{\text{OASPL}}_{\text{duct}}$	overall $\overline{\text{SPL}}_{\text{duct}}$, dB
$\text{OASPL}_{\text{wall}}$	overall SPL_{wall} , dB
PWL	sound-power-level spectrum of noise, dB (ref. 10^{-13} W)
R_1, R_2, R_3	ground reflection reinforcement frequencies, Hz
S/A	treated surface to cross sectional area
SPL	sound pressure level, dB (ref. 2×10^{-5} N/m^2)
$\overline{\text{SPL}}_{\text{duct}}$	average sound-pressure-level spectrum across duct
SPL_{wall}	sound pressure level measured at the suppressor wall, dB
ΔSPL	sound-pressure-level attenuation, dB
s	honeycomb depth or backing distance, m

t	annular gap, m
t_m	thickness of perforated plate, m
θ	angular location of far-field microphones measured from the suppressor inlet, deg
λ	wavelength of sound, m
σ	percent open area of the perforated plate

REFERENCES

1. Feiler, Charles E.; Rice, Edward J.; and Smith, L. Jack: Performance of Inlet Sound Suppressors. Progress of NASA Research Relating to Noise Alleviation of Large Subsonic Jet Aircraft. NASA SP-189, 1968, pp. 53-62.
2. Anon.: NASA Acoustically Treated Nacelle Program. NASA SP-220, 1969.
3. Dorsch, R. G.; Krejsa, E. A.; and Olsen, W. A.: Blown Flap Noise Research. Paper 71-745, AIAA, June 1971.
4. Rice, Edward J.: Propagation of Waves in an Acoustically Lined Duct with Mean Flow. Basic Aerodynamic Noise Research. NASA SP-207, 1969, pp. 345-355.
5. Groeneweg, John F.: Current Understanding of Helmholtz Resonator Arrays as Duct Boundary Conditions. Basic Aerodynamic Noise Research. NASA SP-207, 1969, pp. 356-368.
6. Morse, Philip M.; Ingard, K. Uno: Theoretical Acoustics. McGraw-Hill Book Co., Inc., 1965, pp. 492-522.
7. Beranek, Leo L.: Noise Reduction. McGraw-Hill Book Co., Inc., 1960.
8. Groeneweg, John F.; Feiler, Charles E.; and Acker, Loren W.: Inlet Noise Suppressor Performance Using a Turbojet Engine as a Noise Source. NASA TN D-6395, 1971.
9. Beranek, Leo L.: Acoustics. McGraw-Hill Book Co., Inc., 1954, pp. 268-284.
10. Morse, Philip M.; and Ingard, K. Uno: Theoretical Acoustics. McGraw-Hill Book Co., Inc., 1968, pp. 509-518.
11. Converse, John W.; and Hoffman, Joe D.: Acoustic Standing Waves in a Rocket Combustion Chamber with Ring and Spoke Baffles. Rep. JPC-436, TM-67-5, Purdue Univ. (NASA CR-93262), Aug. 1967.
12. Nagamatsu, H. T.; Sheer, R. E., Jr.; and Horvay, G.: Supersonic Jet Noise Theory and Experiments. Basic Aerodynamic Noise Research. NASA SP-207, 1969, pp. 17-51.



POSTMASTER: If Undeliverable (Section 158
Postal Manual) Do Not Return

"The aeronautical and space activities of the United States shall be conducted so as to contribute . . . to the expansion of human knowledge of phenomena in the atmosphere and space. The Administration shall provide for the widest practicable and appropriate dissemination of information concerning its activities and the results thereof."

—NATIONAL AERONAUTICS AND SPACE ACT OF 1958

NASA SCIENTIFIC AND TECHNICAL PUBLICATIONS

TECHNICAL REPORTS: Scientific and technical information considered important, complete, and a lasting contribution to existing knowledge.

TECHNICAL NOTES: Information less broad in scope but nevertheless of importance as a contribution to existing knowledge.

TECHNICAL MEMORANDUMS: Information receiving limited distribution because of preliminary data, security classification, or other reasons. Also includes conference proceedings with either limited or unlimited distribution.

CONTRACTOR REPORTS: Scientific and technical information generated under a NASA contract or grant and considered an important contribution to existing knowledge.

TECHNICAL TRANSLATIONS: Information published in a foreign language considered to merit NASA distribution in English.

SPECIAL PUBLICATIONS: Information derived from or of value to NASA activities. Publications include final reports of major projects, monographs, data compilations, handbooks, sourcebooks, and special bibliographies.

TECHNOLOGY UTILIZATION PUBLICATIONS: Information on technology used by NASA that may be of particular interest in commercial and other non-aerospace applications. Publications include Tech Briefs, Technology Utilization Reports and Technology Surveys.

Details on the availability of these publications may be obtained from:

**SCIENTIFIC AND TECHNICAL INFORMATION OFFICE
NATIONAL AERONAUTICS AND SPACE ADMINISTRATION
Washington, D.C. 20546**